© Pol J Radiol 2023; 88: e165-e176
DOI: https://doi.org/10.5114/pjr.2023.126251

Received: 30.10.2022
Accepted: 29.12.2022
Published: 28.03.2023

Polish Journal of Radiology

http://www.polradiol.com

Review paper

Pictorial review of computed tomography and magnetic resonance imaging findings of cardiovascular manifestations of IgG4-related disease

Debanjan Nandi[A,B,F], Vineeta Ojha[E,F], Resham Singh[B,F], Sanjeev Kumar[D,F]

Department of Cardiovascular Radiology and Endovascular Interventions, All India Institute of Medical Sciences, New Delhi, India

Abstract

This study includes a series of 5 cases demonstrating cardiovascular manifestations of findings of IgG4-related disease. Two cases demonstrate peri-aortic soft tissue thickening in the infrarenal abdominal aorta and bilateral ostio-proximal common iliac artery. In 2 cases there were circumferential soft tissue lesions around the arch of the aorta. One of the cases showed coexistent, biopsy-proven Riedel's thyroiditis and infiltrative soft tissue along the right atrial wall and interatrial septum. In one case there was a partly calcified mass in the left hemi-thorax consistent with a diagnosis of IgG4-related fibrosing mediastinitis.

Key words: IgG4-related periaortitis, mediastinal fibrosis, cardiovascular manifestations, CT and MRI findings.

Introduction

IgG4 is a multisystem disease with vascular manifestations including aortitis and periaortitis. In a previous study [1] it was reported that 41% of patients who had IgG4-related disease exhibited signs and symptoms of IgG4-related aortitis and/or peri-aortitis, and 80% of these patients had multiple vascular region involvement. The iliac arteries (35% of cases) and infrarenal abdominal aorta (33% of cases) were the most common sites of IgG4-related cardiovascular disease [1]. Radiologically, periaortitis might be distinguished from other large vessel vasculitides because the latter lacks the typical periaortic or perivascular inflammatory cuff that often characterizes periaortitis lesions [2]. IgG4-related disease also causes mediastinal involvement in the form of fibrosing mediastinitis.

Aim

We performed a retrospective review of cases of IgG4-related diseases with cardiovascular involvement with an intent to characterize the extent of disease and involvement of segments of aorta (Table 1).

Methodology

All 5 cases underwent a contrast-enhanced computed tomography study and contrast-enhanced magnetic resonance imaging study. We retrieved the data from departmental PACS and RIS systems. All scans underwent ECG-triggered computed tomography using a third-generation, dual-source, 384-slice machine (CT scanner (DSCT) (SOMATOM Definition Force, Siemens, Erlangen, Germany) and MRI using a 1.5-tesla MRI scanner (MAGNETOM AERA, Siemens).

Case history

Case 1

A 47-year-old male, a shopkeeper by profession, presented with hoarseness of voice for 2 years and atypical chest pain

Correspondence address:
Sanjeev Kumar, Department of Cardiovascular Radiology and Endovascular Interventions, All India Institute of Medical Sciences, New Delhi, India, phone: +9101126593311, e-mail: sanjeevradio@gmail.com

Authors' contribution:
A Study design · **B** Data collection · **C** Statistical analysis · **D** Data interpretation · **E** Manuscript preparation · **F** Literature search · **G** Funds collection

Table 1. Case reports

SR No	Age	Sex	Clinical presentation	Involvement of aorta	Segment of aorta involved	Involvement of pulmonary arteries	Involvement of other arteries	IgG4 level	ESR	CRP	Follow-up
Case 1	47	Male	Hoarseness of voice for 2 years and atypical chest pain for 6 months	Present	Arch of aorta, proximal descending aorta	Absent	Ostioproximal parts of the LCCA and LSCA	2961	50	20	Clinical improvement, no imaging
Case 2	49	Male	Pain abdomen for 3 months	Present	Juxta-renal and infrarenal abdominal aorta	Absent	Bilateral ostio-proximal renal arteries, ostio-proximal inferior mesenteric artery, bilateral ostio-proximal common iliac artery	256	45	43.5	Present
Case 3	20	Male	Heaviness in the chest for 5 months	Present	Aortic arch	Preset, right pulmonary artery	Absent	1040.2	-	-	Present, clinical improvement
Case 4	49	Female	Neck swelling	Present	Arch of aorta and	Present – main pulmonary artery	Ostio-proximal parts of the LCCA and LSC, right coronary artery.	3.31	-	-	Clinical improvement
Case 5	36	Female	Pain abdomen and vomiting from 3 to 4 months	Present	Infrarenal abdominal aorta, just distal to right renal artery origin	Absent	Bilateral ostio-proximal CIA, ostio-proximal IMA	1.932	-	-	Clinical improvement

for 6 months. He had a history of treatment for pulmonary tuberculosis in childhood (10 years of age). He had left-sided vocal cord palsy on a laryngoscopic examination. There were raised inflammatory markers (erythrocyte sedimentation rate [ESR] 50 mm/h [normal range 0-22 mm/h], C-reactive protein [CRP] 20 mg/l [normal range 1-5 mg/l]). Computed angiography revealed circumferential peri-aortic hypodense soft tissue mass encasing the aortic arch, ostio-proximal aortic arch branches, and left pulmonary artery (Figure 1A-B). MRI revealed a lobulated uniformly T1 and T2 hypointense lobulated peri-aortic soft tissue lesion (Figure 2A-B and Figure 3A-C) measuring ~4.3 × 4.7 × 5.2 cm (AP × trans × CC dimensions), encasing arch of aorta, proximal descending aorta, ostio-proximal left common carotid artery, and left subclavian artery. It was indenting the proximal left pulmonary artery (Figure 4A, C) without causing any significant stenosis. No infiltration of adjacent organs, i.e. pulmonary arteries,

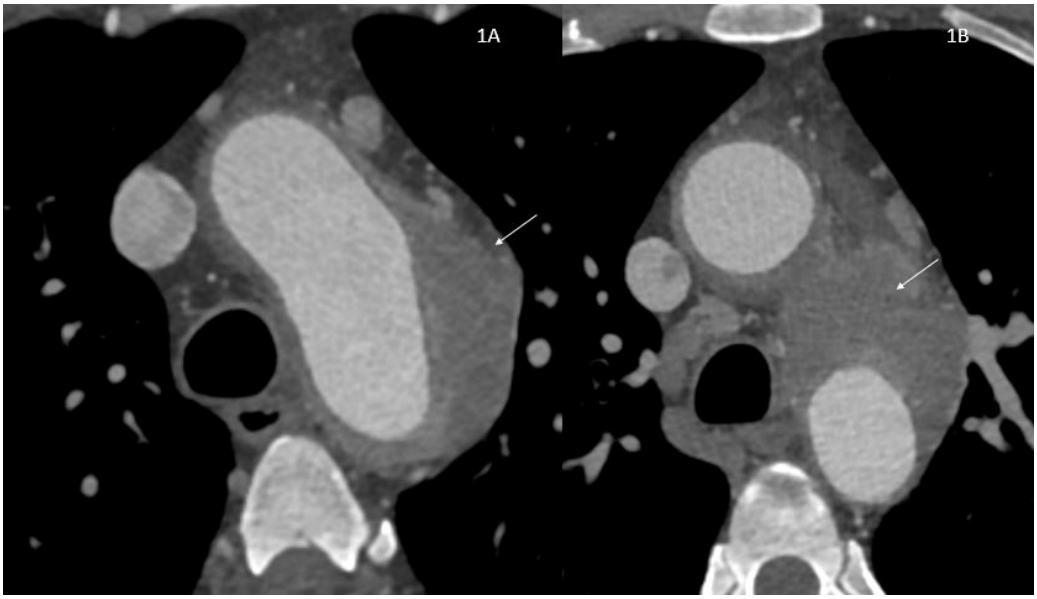

Figure 1. Case 1. Axial computed tomography image shows periaortic soft tissue lesion indicated by white arrow

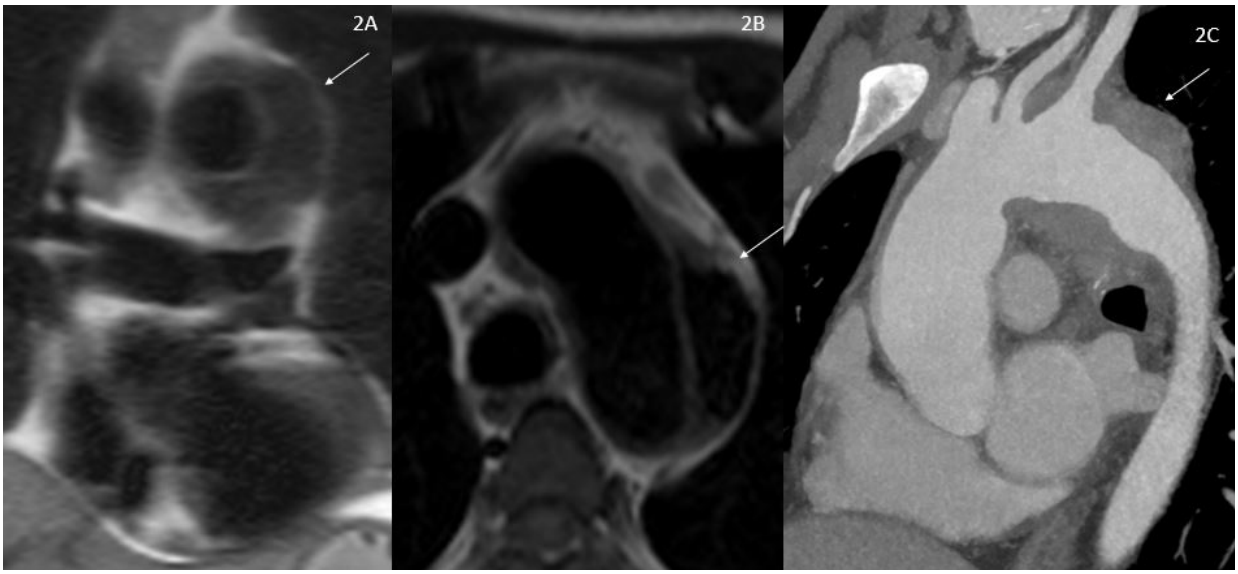

Figure 2. Case 1. **A, B**) Coronal and axial T1W MRI showing hypointense lesion (shown by white arrow) surrounding the aortic arch. **C**) Sagittal computed tomography image showing soft tissue lesion (indicated by white arrow) surrounding the distal arch and proximal descending thoracic aorta

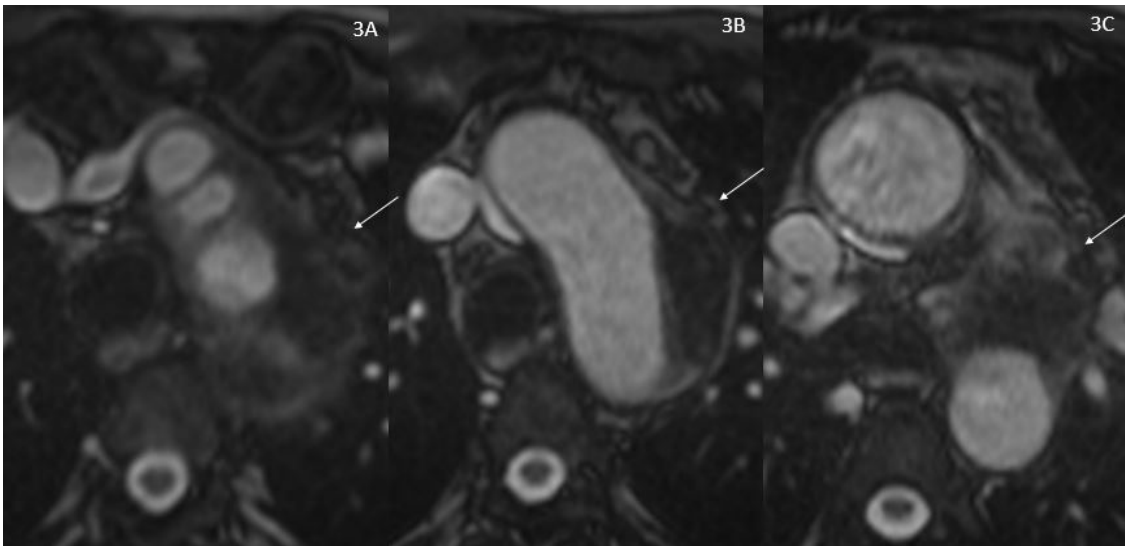

Figure 3. Case 1. Axial T2 images showing hypointense periaortic lesion shown by white arrow

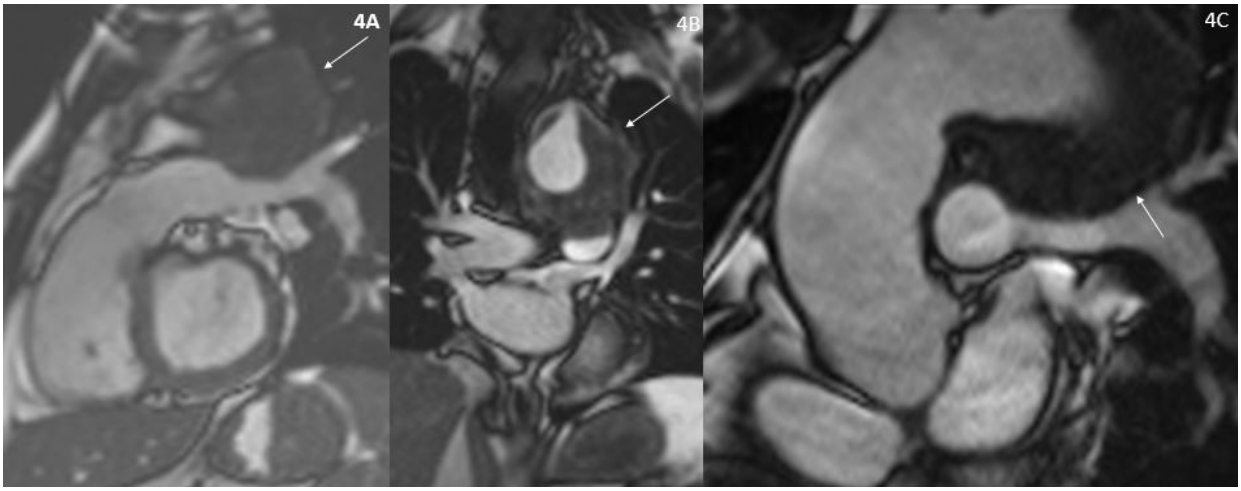

Figure 4. Case **1. A, C**) Sagittal oblique T2 image showing hypointense soft tissue lesion (shown by white arrow) indenting left pulmonary artery. **B**) Coronal T2 image showing soft tissue lesion (shown by white arrow) encasing ostio-proximal left subclavian artery

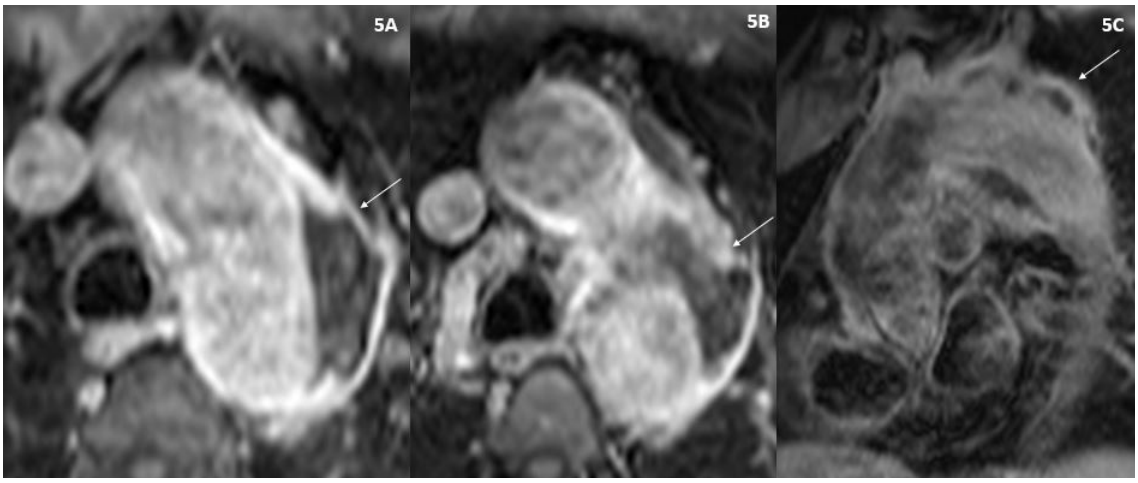

Figure 5. Case 1. **A, B**) Post-contrast axial images showing thin peripheral enhancement of the lesion indicated by white arrow. **C**) Sagittal oblique post-contrast image showing peripheral enhancement

trachea, oesophagus, was seen. Thin peripheral rim enhancement of the mass was seen in post-contrast images (Figure 5A-C). No mediastinal adenopathy or pleural/pericardial effusion was seen. Endobronchial ultrasound revealed possible organized haematoma. On echocardiography, biventricular functions were normal. There was increased globulin – 5 g/dl (normal range – 3-3.7 g/dl) with albumin; the globulin ratio was low (0.8). The IgG4 level was 2961 mg/dl (700-1600), lymphocytic Abs– 4.05×10^3 [1-3]. Differentials to be considered in this case were IgG4-related peri-aortitis tubercular peri-aortitis, organized haematoma, thrombosed pseudoaneurysm, lymphoma, and histiocytosis (Erdheim-Chester) disease. However, given the raised serum IgG4 levels, a diagnosis of IgG4-related peri-aortitis was considered. The patient was started on steroids. A follow-up examination revealed significant clinical improvement.

Case 2

A 49-year-old male presented with pain in the abdomen for 3 months. Contrast-enhanced computed tomography of the abdomen revealed enhancing soft tissue thickening along the infra-renal abdominal aorta (Figure 6A and Figure 7A-B). MRI and MR angiography revealed circumferential lobulated periaortic soft tissue thickening (maximum thickness

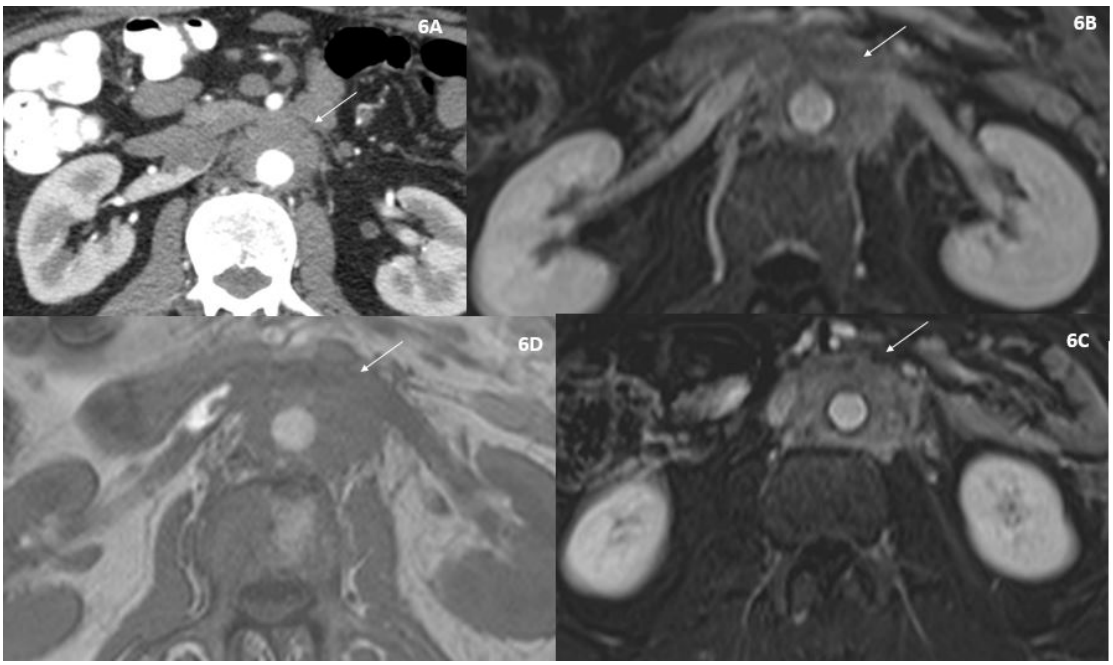

Figure 6. Case 2. Pre-steroid treatment images. **A**) Pretreatment axial computed tomography image showing soft tissue thickening (indicated by white arrow) along abdominal aorta with encasement of right renal vein. **B, C**) Pretreatment axial post-contrast image showing soft tissue thickening (indicted by white arrow) encasement of proximal segments of both renal arteries and veins. **D**) Pretreatment Axial T1W MRI image showing T1 hypointense soft tissue thickening indicated by white arrow

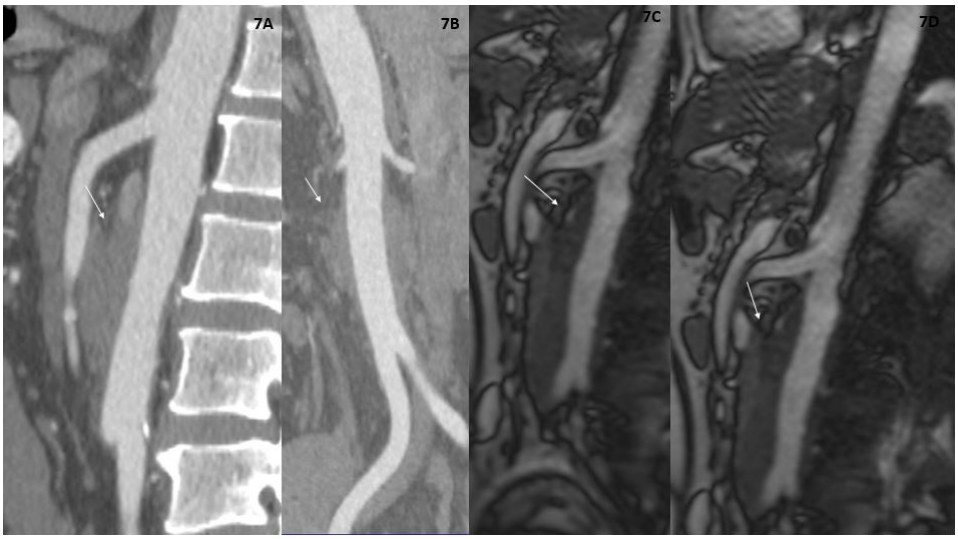

Figure 7. Case 2. Pre-steroid treatment images. **A, B**) Pretreatment sagittal and coronal oblique post-contrast CT image showing soft tissue thickening along infrarenal abdominal aorta indicated by white arrow. **C, D**) Pretreatment Sagittal T2W MRI image showing soft tissue thickening along infrarenal abdominal aorta indicated by white arrow

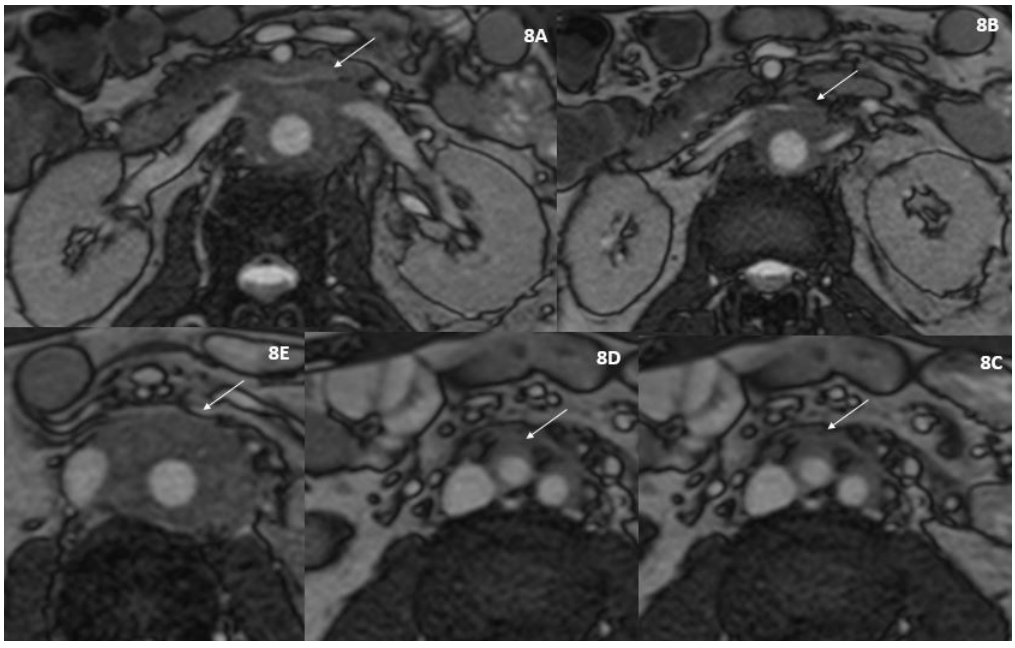

Figure 8. Case 2. Pre-steroid treatment images. Pretreatment axial T2 image showing soft tissue thickening along infrarenal abdominal aorta and also extending to encase bilateral common iliac arteries

~22 mm) involving juxta-renal and infra-renal abdominal aorta up to bilateral ostio-proximal common iliac artery. The soft tissue thickening was T1 hypointense (Figure 6D), heterogeneously T2 hypointense (Figure 8A-D and Figure 7C), and showed enhancement on delayed (10 and 15 min) post-contrast images (Figure 6B-C and Figure 9). It partially encased the inferior vena cava (Figure 8A) and encased the bilateral ostio-proximal renal arteries (Figure 8B) and veins (Figure 6B and Figure 8A). No significant retroperitoneal and mesenteric adenopathy was present. There were raised inflammatory markers, i.e ESR (45), CRP (43.5), and ferritin (177.9). The A/G ratio was 1.6 (normal rage 0.8-2.0). Normal biventricular functions were demonstrated on echocardiography. IgG4 levels were elevated at 256 mg/dl. Given th4 raised IgG4 level and typical location of periaortic soft tissue thickening, a diagnosis of IgG4-related peri-aortitis was made. The patient was started on steroids. On follow-up examination after 3 months, there was resolution of abdominal pain and follow-up MRI revealed a significant decrease in thickening and enhancement of the periaortic soft tissue lesion, the maximum thickness now measuring ~1 cm.

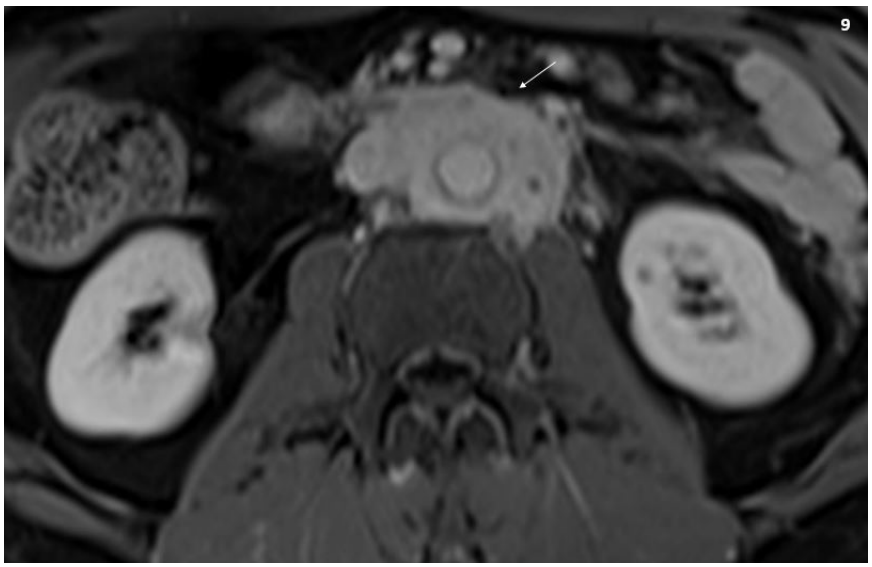

Figure 9. Case 2. Pre-steroid treatment images. Pretreatment axial post-contrast image showing intense enhancement of the lesion

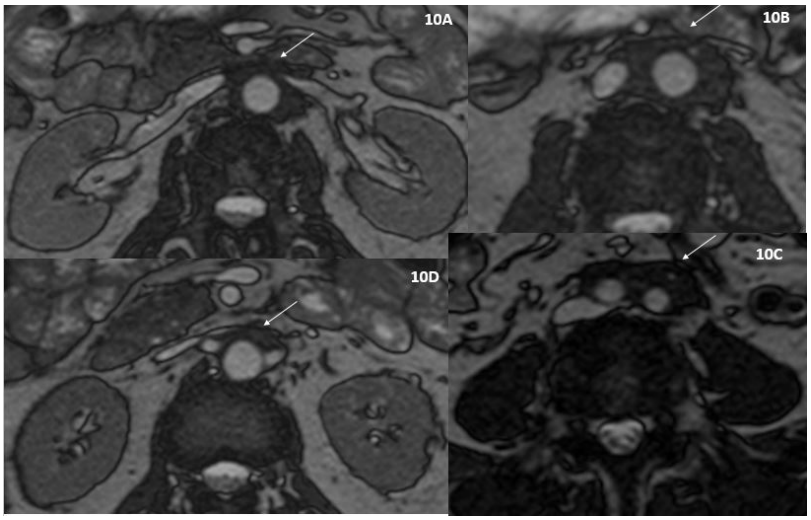

Figure 10. Case 2. Post-steroid therapy. Post-treatment axial T2 image showing decrease in size of the lesion

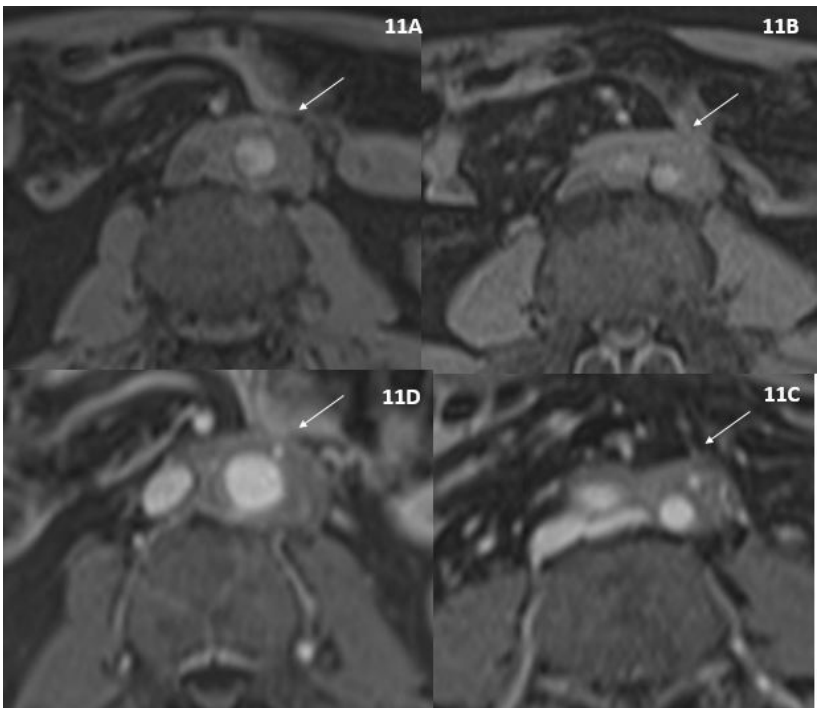

Figure 11. Case 2. Post-steroid therapy. Post-treatment axial post contrast image showing decrease in intensity of enhancement of the lesion

Case 3

A 20-year-old man presented with heaviness in his chest for 5 months. There was no history of tuberculosis or travel history to a histoplasmosis endemic area. Computed tomography in the arterial and venous phase revealed a large multilobulated, heavily calcified mass in the left hemi-thorax (Figure 12A-C). Contrast enhanced cardiac MRI revealed heterogeneous peripheral enhancement with central non-enhancing areas. The mass involved the parietal pericardium along the left cardiac border and posterior atrioventricular groove with moderate pericardial effusion (Figure 13A, D). The LV free wall appeared uninvolved. The mass was encasing the left atrium and left side pulmonary veins. The left pulmonary artery and its branches were encased and narrowed. The mass had a broad area of contact with the anterior and lateral left chest wall with no definite chest wall invasion seen. No mediastinal lymphadenopathy was seen. A/G ratio was 0.77. CT-guided biopsy from the mass was consistent with diagnosis of fibrosing mediastinitis. The serum IgG4 level was 1040.2 mg/dl. Diagnosis of IgG4 related fibrosing mediastinitis was made and the patient improved clinically with steroid therapy followed by surgical resection.

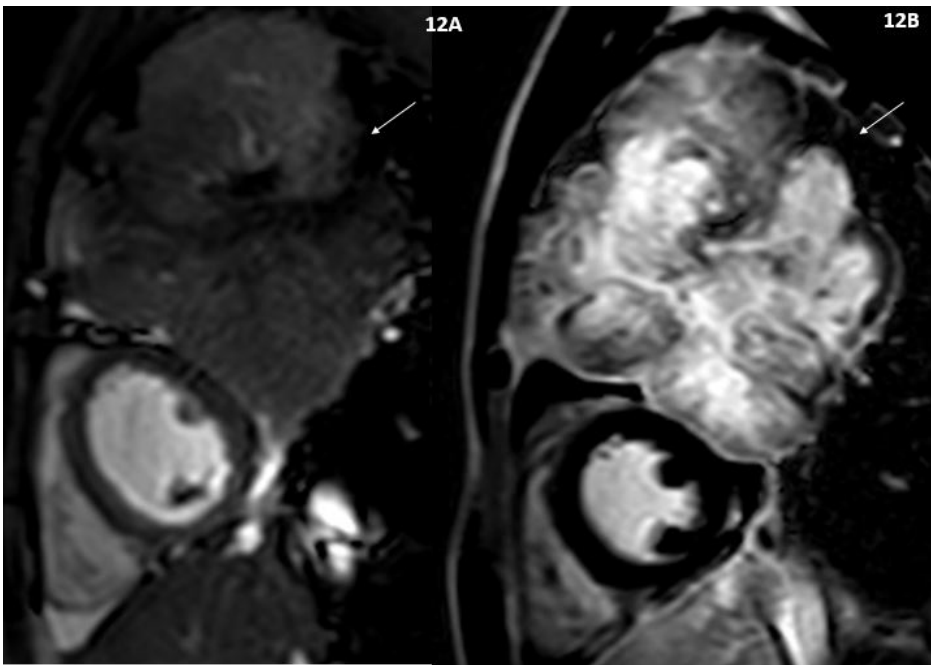

Figure 12. Case 3. **A**) Short-axis T2 image showing lobulated T2 heterogeneously hypointense lesion with involvement of parietal pericardium and abutment of LV myocardium. **B**) Short-axis post-contrast image showing heterogeneous post-contrast enhancement of the lesion

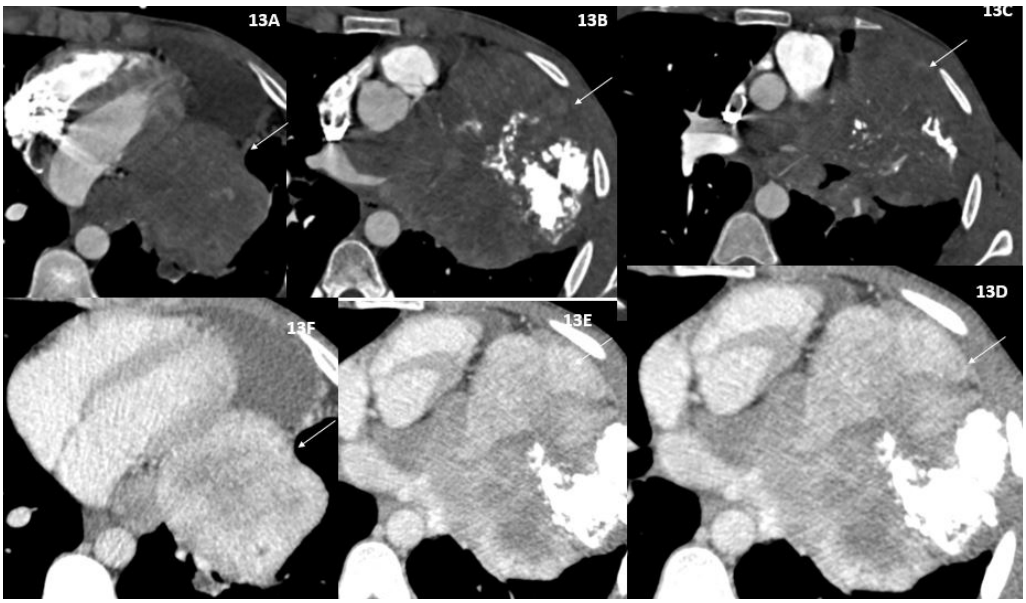

Figure 13. Case 3. **A-C**) 4-chamber arterial phase CT images show calcification within the mass in the left hemi-thorax and extension to the antero-lateral chest wall. **D-F**) 4-chamber arterial phase CT images show heterogenous post-contrast enhancement of the mass in left hemithorax

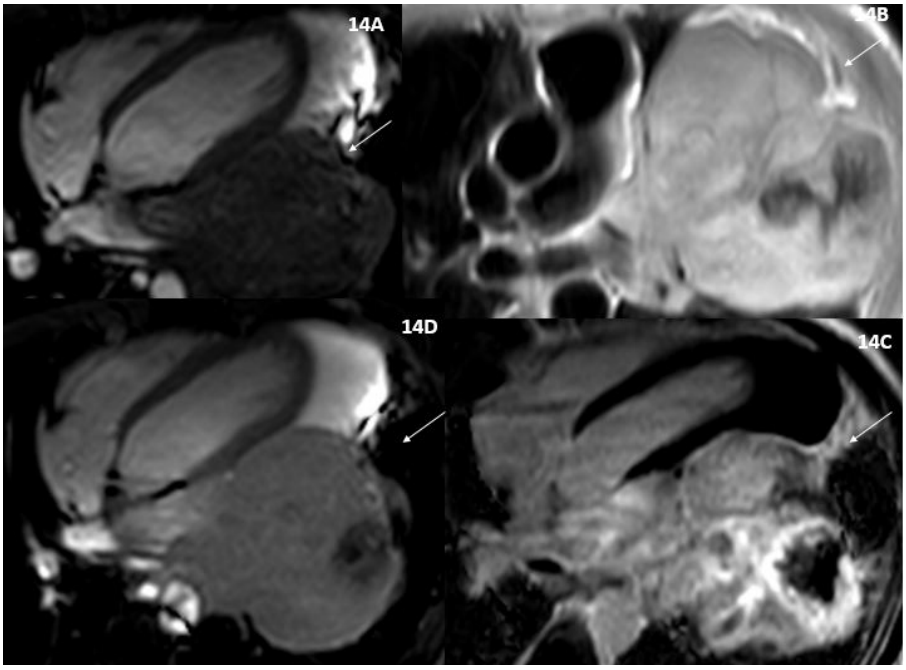

Figure 14. Case 3. 4-chamber bright blood (**A, D**) image showing T1 hypointense (**A**) and T2 hyperintense (**D**) mass lesion. **B**) Black blood image showing hyperintense mass abutting pericardium. **D**) LGE image showing heterogenous enhancement of the mass with few non-enhancing areas consistent with the calcification

Case 4

A 49-year-old female complained of neck swelling for one year. Anteroposterior chest radiograph revealed significant pericardial effusion (Figure 15). Ultrasound neck revealed diffuse heterogeneous echotexture and enlarged thyroid gland with mildly increased vascularity (Figure 17C, D and Figure 20B). A biopsy from the thyroid nodule revealed Riedel's thyroiditis with infiltration by immunoglobulin 4 (IgG4)-positive plasma cells. Computed tomography of the thorax, abdomen, and pelvis and contrast-enhanced MRI and neck ultrasound revealed a diffusely enlarged thyroid gland (Figure 18A). The circumferential soft tissue lesion in the superior mediastinum was encasing the arch of the aorta (Figure 16A) and main pulmonary artery, extending to the bilateral hilum AP window region and along the right atrial wall, interatrial septum, and the wall of the superior and inferior vena cava (Figure 18B, D-F) causing luminal narrowing of the right atrium and SVC-right atrial junction (Figure 18 E, F) and IVC (Figure 19A). The lesion encased the right coronary artery (Figure 16D, E). CT-guided biopsy from the anterior mediastinal lesion revealed fibro-collagenous tissue with mild chronic inflammation. The albumin : globulin ratio was 1.35, and the serum IgG4 level was 3.31 g/l (normal range 0.03-2.01 g/l). T4 was 7.93 µg/dl, and TSH was decreased, at 0.2258 uIU/ml. The patient was started on steroids, with significant clinical improvement, as well as echocardiography.

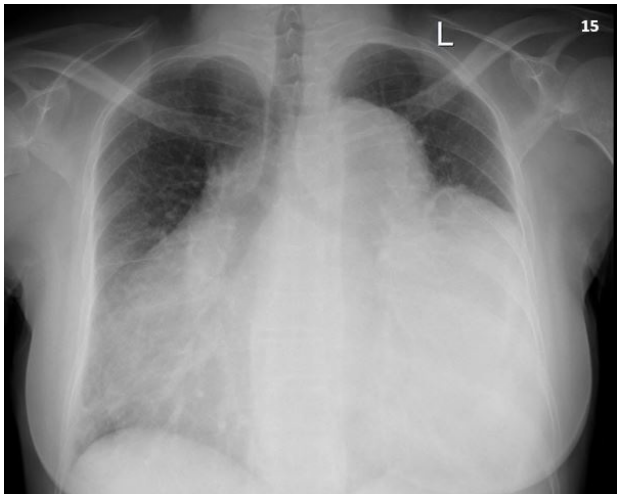

Figure 15. Case 4. Anteroposterior chest radiograph pericardial effusion

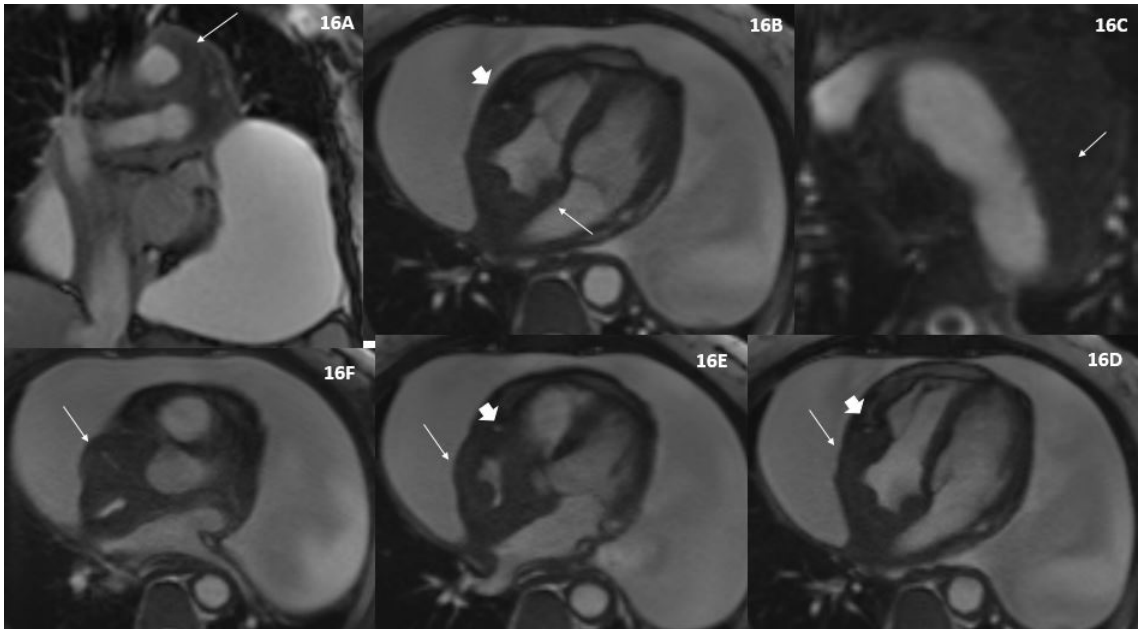

Figure 16. Case 4. **A**) Coronal T2 image showing T2 hypointense soft tissue lesion encasing aortic arch. **B, D-F**) Axial 4-chamber image showing T2 hypointense atrial wall thickening, interatrial septum thickening, thickening along SVC, IVC with encasement of right coronary artery (indicated by thick arrow)

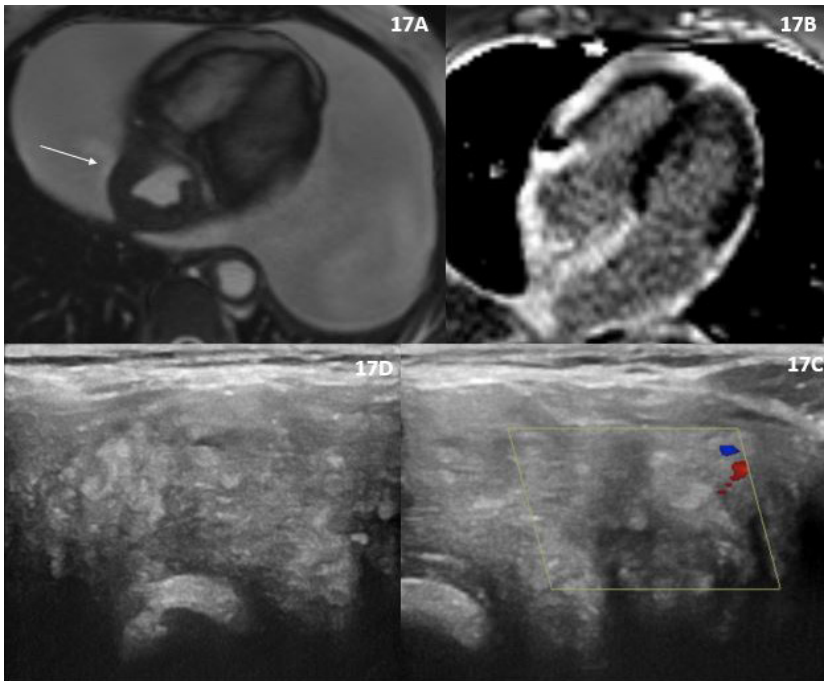

Figure 17. Case 4. **A**) Axial 4-chamber image showing T2 hypointense atrial wall thickening, interatrial septum thickening, thickening along SVC, IVC with encasement of right coronary artery (indicated by thick arrow). **B**) 4-chamber post-contrast image showing intense late gadolinium enhancement along atrial wall thickening. **C, D**) USG image showing heterogenous echotexture of enlarged thyroid gland with mild increased vascularity

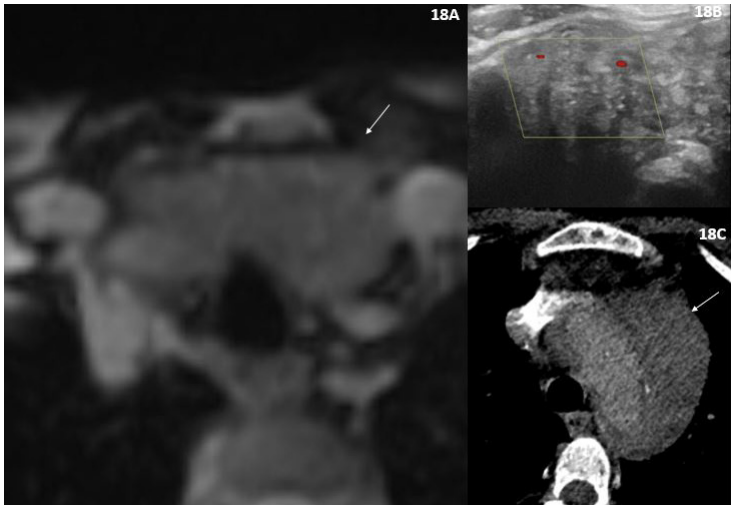

Figure 18. Case 4. **A**) Enlarged thyroid gland with mediastinal extension shown in post-contrast MRI images. **B**) USG image showing heterogenous echotexture of enlarged thyroid gland with mild increased vascularity. **C**) Periaortic soft tissue lesion along the aortic arch in post-contrast CT image

Case 5

A 36-year-old woman presented with pain in the abdomen and vomiting for 4 months. History of surgery for a left adnexal mass with adhesions in the posterior wall of the uterus 7 years previously and hysterectomy 5 years ago. Computed tomography of the abdomen and contrast-enhanced MRI and MR angiography revealed circumferential homogeneously enhancing peri-aortic soft tissue thickening (maximum thickness: 5 mm) encasing infrarenal abdominal aorta, and bilateral ostio-proximal common iliac artery (Figure 19 A-C, E). The ostio-proximal inferior mesenteric artery was also encased. This caused minimal luminal narrowing of the infrarenal aorta (Figure 19D) and bilateral ostio-proximal CIA and mild luminal narrowing of the ostio-proximal IMA (~50%) (Figure 20B). This thickening was iso- to hypointense on T1 and T2 and showed post-contrast enhancement. There was no significant retroperitoneal and mesenteric lymphadenopathy. The albumin : globulin ratio was 1.5. Serum IgG was elevated, at 1.932 mg/dl (normal: 0.1-1.2).

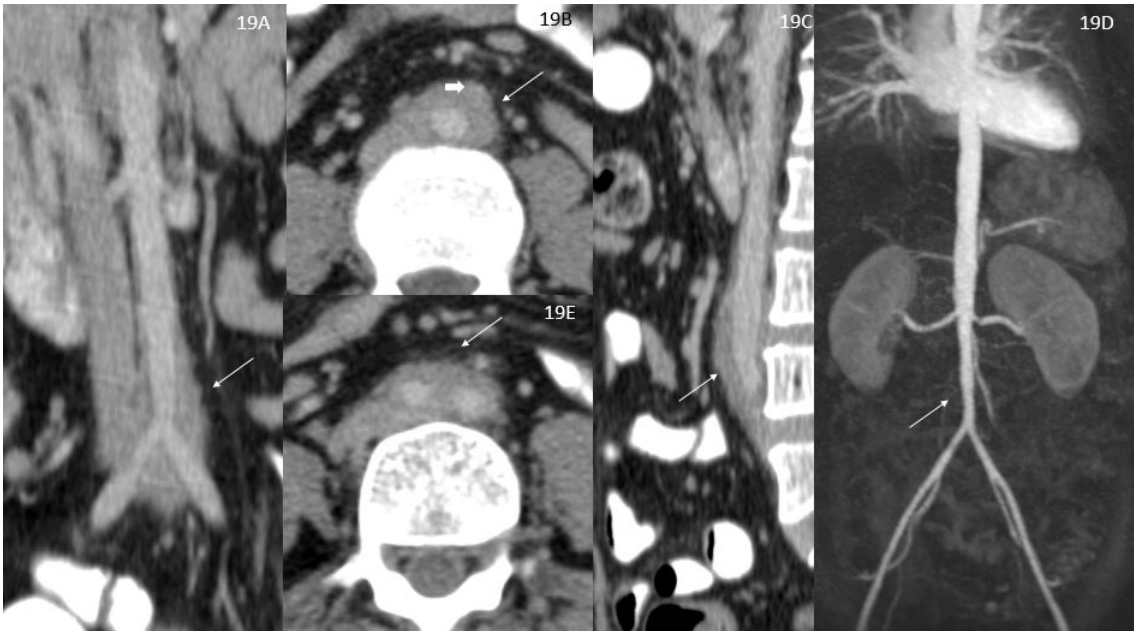

Figure 19. Case 5. **A-C, E**) Computed tomography image showing soft tissue thickening (indicated by white arrow) along abdominal aorta. **D**) Coronal MRI angiography revealed mild narrowing of infrarenal abdominal aorta

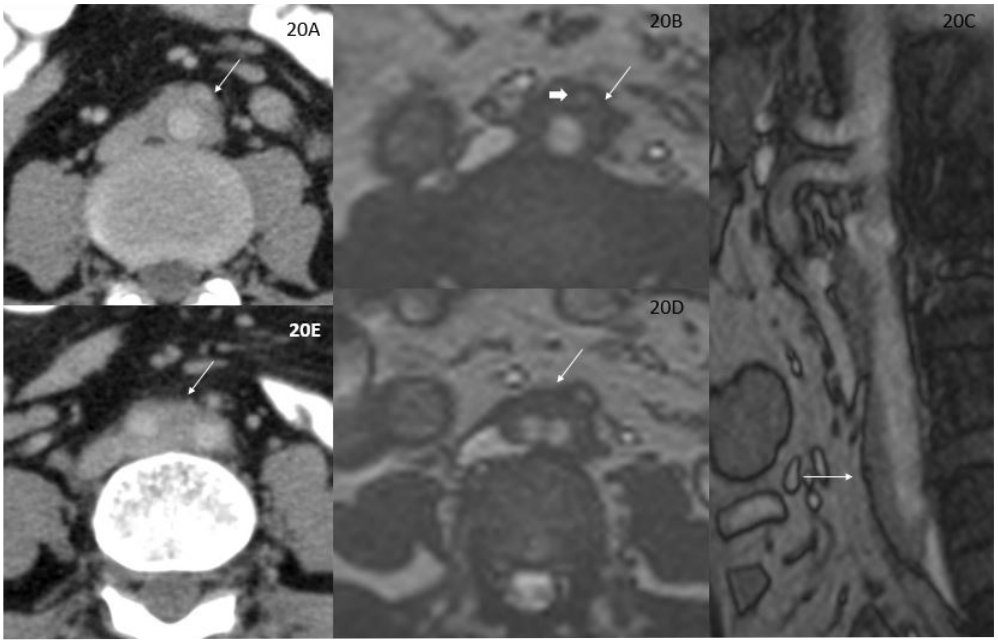

Figure 20. Case 5. **A, E**) Computed tomography image showing soft tissue thickening (indicated by white arrow) along abdominal aorta. **B, C, D**) Axial and sagittal T2W image showing soft tissue thickening (indicated by white arrow) along abdominal aorta with encasement of inferior mesenteric artery shown by a thick arrow

Discussion

In this case series, the mean age was 40.2 (range 20-49) years, with 4 male subjects and only one female subject – consistent with the fact that IgG4-related disease is more common among elderly males compared to Takayasu arteritis, which is more common among young females.

In this above series, cases 1, 3, and 4 presented with intrathoracic masses, whereas cases 2 and 5 presented with wall thickening along the abdominal aorta. For case 1, 3 possible differential diagnoses including lymphoma and thymoma should be considered. Case 3 was diagnosed as IgG4-related fibrosing mediastinitis – a subset of non-granulomatous fibrosing mediastinitis. None of the cases had an aneurysm or significant stenosis of the vessel. Case 4 had right coronary artery involvement in the form of pseudotumor formation.

Two cases, i.e. case 3 and case 4, had pulmonary artery involvement; in case 1, there was indentation of the left pulmonary artery. Both case 2 and case 5 had ostio-proximal common iliac artery involvement and encasement of the inferior mesenteric artery, with case 2 having bilateral ostio-proximal renal artery involvement. There was no hydroureteronephrosis in these cases, as sometimes found in IgG4-related idiopathic retroperitoneal fibrosis cases. Both case 1 and case 4 had involvement of the bilateral ostio-proximal left common carotid artery and left subclavian artery.

Two patients in whom ESR and CRP levels were available, i.e cases 1 and 2, had raised ESR and CRP, which are considered useful markers for the inflammatory activity of IgG4-related disease.

Previous literature revealed that IgG4-related disease generally presents with normal CRP levels [3]. Some forms of IgG4-related disease, such as IgG4-related retroperitoneal fibrosis, periaortitis, inflammatory aortic aneurysms, and fibrosing mediastinitis, can present with high serum CRP [4].

IgG4-related disease is accompanied by a decreased albumin : globulin (A/G) ratio, which reflects the overproduction of immunoglobulin; therefore, it is useful for simplified screening and follow-up of IgG4-related disease patients. In this case series the mean albumin : globulin ratio was 1.2 (0.8, 1.6, 0.77, 1.35, 1.5).

Other cardiovascular involvement of IgG4-related disease ranges from abdominal aortic aneurysm, thoracic aortic aneurysm, coronary aneurysm, aneurysm of other arteries (constrictive pericarditis), and pseudo-tumours around coronary arteries [6]. IgG4-positive plasma cell infiltration into pericardium can cause IgG4-related constrictive pericarditis. Most cases of IgG4-related aneurysm and aortitis show IgG4-positive cell and eosinophil infiltration in adventitia, but some cases also show them in intima in addition to the adventitia. Therefore, aneurysm formation might follow aortitis or arteritis. The thickened inflammatory aneurysmal wall protects itself from rupture risk and corticosteroid therapy may increase rupture risk by weakening the aneurysmal wall.

Diagnosis

Characteristic diffuse/localized swelling in one or more organs at clinical examination, increased serum IgG4 level (≥ 135 mg/dl [≥ 1.35 g/l]) at the haematological examination, marked lymphoplasmacytic infiltration, and storiform fibrosis with organ infiltration by IgG4-positive plasma cells at the histopathologic examination were present in IgG4-related disease. The diagnosis of IgG4-related disease is considered to be definite when all these 3 criteria are fulfilled, probable when the first and third criteria are satisfied, and possible when only the first and second criteria are met [5].

In the case of periaortitis/periarteritis, other differential diagnoses, i.e giant cell arteritis, Takayasu arteritis, rheumatoid arthritis, systemic lupus erythematosus (SLE), HLA-B27-associated spondyloarthropathies, ANCA-associated vasculitides, and Behçet disease should also be considered [6].

Histopathological analysis in IgG4-related peri-aortitis/periarteritis reveals inflammatory infiltrates in the adventitia, while they were seen in the medial layer in giant cell arteritis and the medial layer to adventitia in Takayasu arteritis and SLE-associated arteritis.

Conclusions

These cases demonstrate that cardiovascular manifestations of IgG4-related disease were diverse, ranging from typical peri-aortitis of the abdominal aorta to fibrosing mediastinitis with adjacent pericardial involvement, intracardiac involvement in the form of atrial wall thickening, and pseudotumour around the coronary artery. The albumin:globulin ratio can be normal in such cases. Because IgG4-related cardiovascular disorder affects prognosis, early detection and treatment are important. Corticosteroids suppress the development of active inflammatory diseases such as aortitis, pericarditis, and pseudotumours, but lesions with predominant fibrosis may need surgical resection in view of less response to corticosteroids.

Disclosure

The authors report no conflict of interest.

References

1. Yabusaki S, Oyama-Manabe N, Manabe O, et al. Characteristics of immunoglobulin G4-related aortitis/periaortitis and periarteritis on fluorodeoxyglucose positron emission tomography/computed tomography co-registered with contrast-enhanced computed tomography. EJNMMI Res 2017; 7: 20. doi: 10.1186/s13550-017-0268-1.
2. Vaglio A, Pipitone N, Salvarani C. Chronic periaortitis: a large-vessel vasculitis? Curr Opin Rheumatol 2011; 23: 1-6.
3. Sasaki T, Akiyama M, Kaneko Y, et al. Distinct features distinguishing IgG4-related disease from multicentric Castleman's disease. RMD Open 2017; 3: e000432. doi: 10.1136/rmdopen-2017-000432.
4. Takanashi S, Akiyama M, Suzuki K, et al. IgG4-related fibrosing mediastinitis diagnosed with computed tomography-guided percutaneous needle biopsy: two case reports and a review of the literature. Medicine (Baltimore) 2018; 97: e10935. doi: 10.1097/MD.0000000000010935.
5. Umehara H, Okazaki K, Masaki Y, et al. Comprehensive diagnostic criteria for IgG4-related disease (IgG4-RD), 2011. Modern Rheumatology 2012; 22: 21-30.
6. Oyama-Manabe N, Yabusaki S, Manabe O, et al. IgG4-related cardiovascular disease from the aorta to the coronary arteries: multidetector CT and PET/CT. Radiographics 2018; 38: 1934-1948.